Proceedings of the 35th Chinese Control Conference
July 27-29, 2016, Chengdu, China

Quaternion-Based Robust Extended Kalman Filter for Attitude Estimation of Micro Quadrotors Using Low-cost MEMS

Li Xiaoran, Chen Mou, Zhang Lei

College of Automation Engineering, Nanjing University of Aeronautics and Astronautics, Nanjing, 210016
E-mail: lixiaoran@nuaa.edu.cn, chenmou@nuaa.edu.cn, 1139298349@qq.com

Abstract: In this paper, a quaternion-based robust extended Kalman filter (EKF) is developed for the attitude estimation of micro quadrotors. Since the raw data of low-cost MEMS is sensitive to the environmental conditions, the attitude estimation method is developed to minimize the influence of outlier and to estimate the bias effectively. In order to overcome the singularity of certain orientation, the quaternion is involved in the filter parameter. A cortex-M4 based micro quadrotor is developed to implement the proposed quaternion-based robust extended Kalman filter, and simulation results show good estimation accuracy and satisfactory real-time performance.

Key Words: Attitude estimation; Extended Kalman Filter; Low-cost MEMS; Micro Quadrotor, Quaternion

1 Introduction

Since the attitude estimation can provide the essential information to stabilize flight state, it is a prerequisite for precise control of micro quadrotors. Without reliable attitude information, the micro quadrotor cannot flight well or even be unstable.

There is no explicit classification of micro quadrotor, but its size could be around 10 cm and with a mass of around 30g [1]. Because of the small size of micro quadrotor, it can operate in a confined narrow space and easily land on small surface. Thus, the micro quadrotor has great potential in fault detection, rescue and so on. The same as many unmanned aerial vehicles (UAV) having on-board control system, the micro quadrotor usually includes microprogramme control unit (MCU), inertial measurement unit (IMU), and other circuits in just a small chip. Along with the development of IMU, low-cost micro electro mechanical systems (MEMS) sensors have enabled the microminiaturization of quadrotor. However, this may lead to some problems. On the one hand, scaling down the size improves its agility but requires a short control period. Thus, the attitude estimation algorithm should be faster. On the other hand, low-cost MEMS sensors always have bias and the error drift with time. Thus, the attitude estimation algorithm must reduce the error effectively.

Kalman filter is a well-known attitude estimation algorithm, and many improved Kalman filters have been developed over the past years. In [2], an improved quaternion based extend Kalman filter (EKF) was developed based on the data obtained from a tri-axis accelerometer, a tri-axis accelerometer and a tri-axis magnetometer, which can deal with the time-varying biases and disturbances well. However, the linearization in EKF can bring a large residual [3]. In [4], the Unscented Kalman Filter (UKF) was proposed by Julier and Uhlamn. The UKF was used in attitude estimation, and simulation results indicated that the performance of UKF is far better than EKF under large initialization errors in [5]. However, the conversion between quaternion and Rodrigues parameters increased the complexity of the algorithm.

Considering the outliers of raw data, an efficient robust Kalman filter was proposed in [6]. In [7], the robust Kalman filter was designed using Bayesian statics and a robust M-estimate, and the outliers were involved in both observations and updated parameters. In [8], a robust extended Kalman filter was derived to tackle the motion disturbances and magnetic disturbances, and the experimental results on a self-designed quadrotor showed a good real-time performance. However, the Kalman filter depends on Euler angles suffers from singularities in certain orientations [9].

In this paper, we develop a quaternion-based robust extended Kalman filter with the following features: instead of Euler angles, both quaternion and the bias of accelerometer and magnetometer are involved in state equation, which can overcome the singularity and estimate the bias of sensors to compensate for it in the meantime. A weight matrix is introduced to adjust the covariance matrix of observation noise. As a result, the outlier in observation is controlled. Considering the earth field is variable in different latitude, longitude and elevation, the horizon output of magnetometer is calibrated to guarantee the accuracy of yaw angle. Because of the limit compute capacity of MCU, a special digital signal processing (DSP) library is adopted to carry out the method, which is more than 10 times faster than the common math libraries; A 9-axis IMU, including a tri-axis gyroscope, a tri-axis accelerometer and a tri-axis magnetometer, is integrated in the self-designed micro quadrotor, which has a better coaxiality than using discrete devices.

2 Quaternion and Orientation Representation

For the further derivation, basic concepts of quaternion and rotation are presented in this section. A quaternion is a hyper complex number which can be in different forms. In this paper, we denote a quaternion as follows [2]:

$$\begin{aligned} q &= [q_0 \quad q_1 \quad q_2 \quad q_3]^T \\ &= [q_0 \quad e]^T \end{aligned} \tag{1}$$

* This work is supported by National Natural Science Foundations of China (No. 61533008, 61573184), and Specialized Research Fund for the Doctoral Program of Higher Education (Granted Number: 0133218110013).

where q_0 is the scalar part and $e=\begin{bmatrix} q_1 & q_2 & q_3 \end{bmatrix}$ is the vector part.

The rotation form the navigation frame (denote n) to the body frame (denote b) can be expressed as [2]:

$$X^b(t)=C_n^b(q)X^n(t) \tag{2}$$

where $X^b(t)$, $X^n(t)$ are vectors in frame b and frame n respectively. $C_n^b(q)$ is the direction cosine matrix (DCM). $C_n^b(q)$ at any $t>0$ can be determined by solving the direction cosine matrix differential equation. However, the calculation burden is large. Thus, $C_n^b(q)$ is obtained from the quaternion [2]:

$$C_n^b(q)=\begin{bmatrix} q_0^2+q_1^2-q_2^2-q_3^2 & 2(q_1q_2+q_3q_0) & 2(q_1q_3-q_2q_0) \\ 2(q_1q_2-q_3q_0) & q_0^2-q_1^2+q_2^2-q_3^2 & 2(q_2q_3+q_0q_1) \\ 2(q_1q_3+q_2q_0) & 2(q_2q_3-q_0q_1) & q_0^2-q_1^2-q_2^2+q_3^2 \end{bmatrix} \tag{3}$$

where we assume that $|q|=1$.

Differentiating the quaternion yields

$$\frac{d}{dt}q=\frac{1}{2}\Omega(\omega)q \tag{4}$$

where $\Omega(\omega)=\begin{bmatrix} 0 & -\omega \\ \omega^T & -[\omega\times] \end{bmatrix}$, $\omega=\begin{bmatrix} \omega_x & \omega_y & \omega_z \end{bmatrix}^T$ is the angular velocity vector of the body frame with respect to navigation frame. $[\omega\times]$ is the cross product matrix which is defined as

$$[\omega\times]=\begin{bmatrix} 0 & -\omega_z & \omega_y \\ \omega_z & 0 & -\omega_x \\ -\omega_y & \omega_x & 0 \end{bmatrix} \tag{5}$$

The discrete form of (4) is given by

$$q(k+1)=\exp(\Omega(k)T_s)q(k),\ k=0,1,\cdots \tag{6}$$

where T_s is the sampling interval.

The calculation of exponential $\exp(\Omega(k)T_s)$ or solving the differential equation is impracticable in MCU programming. Therefore, we introduce the Picard method to discretize equation (4) as [10]

$$q(k+1)=\varphi(k)q(k),\ k=0,1,\cdots \tag{7}$$

where

$$\varphi(k)=\begin{bmatrix} 1-\frac{\Delta\theta_0^2}{8}+\frac{\Delta\theta_0^4}{384} & -(\frac{1}{2}-\frac{\Delta\theta_0^2}{48})\Delta\theta_x & -(\frac{1}{2}-\frac{\Delta\theta_0^2}{48})\Delta\theta_y & -(\frac{1}{2}-\frac{\Delta\theta_0^2}{48})\Delta\theta_z \\ (\frac{1}{2}-\frac{\Delta\theta_0^2}{48})\Delta\theta_x & 1-\frac{\Delta\theta_0^2}{8}+\frac{\Delta\theta_0^4}{384} & (\frac{1}{2}-\frac{\Delta\theta_0^2}{48})\Delta\theta_z & -(\frac{1}{2}-\frac{\Delta\theta_0^2}{48})\Delta\theta_y \\ (\frac{1}{2}-\frac{\Delta\theta_0^2}{48})\Delta\theta_y & -(\frac{1}{2}-\frac{\Delta\theta_0^2}{48})\Delta\theta_z & 1-\frac{\Delta\theta_0^2}{8}+\frac{\Delta\theta_0^4}{384} & (\frac{1}{2}-\frac{\Delta\theta_0^2}{48})\Delta\theta_x \\ (\frac{1}{2}-\frac{\Delta\theta_0^2}{48})\Delta\theta_z & (\frac{1}{2}-\frac{\Delta\theta_0^2}{48})\Delta\theta_y & -(\frac{1}{2}-\frac{\Delta\theta_0^2}{48})\Delta\theta_x & 1-\frac{\Delta\theta_0^2}{8}+\frac{\Delta\theta_0^4}{384} \end{bmatrix} \tag{8}$$

The initial quaternion can be determined as $q(0)=[1\ \ 0\ \ 0\ \ 0]^T$, and if T_s is short enough, ω_k can be regarded as a constant over the interval. Then, $\Delta\theta_x=\omega_xT_s$, $\Delta\theta_y=\omega_yT_s$, $\Delta\theta_z=\omega_zT_s$, $\Delta\theta_0^2=\Delta\theta_x^2+\Delta\theta_y^2+\Delta\theta_z^2$.

In the update of quaternion, no trigonometric function is used and no singularity exists. Considering the expect input is Euler angles, the transform between quaternion and Euler angles is given by [11]

$$\begin{aligned} \theta &= -\text{asin}[2(q_1q_3-q_0q_2)] \\ \varphi &= \text{atan}\,2\left[\frac{2(q_2q_3+q_0q_1)}{q_3^2-q_2^2-q_1^2+q_0^2}\right] \\ \psi &= \text{atan}\,2\left[\frac{2(q_1q_2+q_0q_3)}{q_0^2+q_1^2-q_2^2-q_3^2}\right] \end{aligned} \tag{9}$$

3 System Modeling

3.1 Sensor Model

The gyroscope, accelerometer and magnetometer are equipped sensors to provide raw data for attitude estimation. They are fixed on the flight control board in specific direction according to body frame.

Considering that there exist bias and noise of low-cost MEMS, the sensors can be modeled as:

$$\begin{cases} \omega_{ob}=\omega+b_g+\eta_g \\ a_{ob}=C_n^b(q)(a+a_l)+b_a+\eta_a \\ m_{ob}=C_n^b(q)m+b_m+\eta_m \end{cases} \tag{10}$$

where ω_{ob} , a_{ob} , m_{ob} are observed values of sensors; ω , a , m are the true values; a_l denotes the linear acceleration ($a_l\approx 0$); b_g , b_a , b_m are bias vectors; η_g , η_a , η_m are independent white Gaussian measurement noise with zero mean value and their covariance matrices are σ_g^2I , σ_a^2I , σ_m^2I , respectively.

The sensors, especially the gyroscope, are sensitive to the environmental conditions. Take the MPU9150 gyroscope as an example, the error of gyroscope results from many factors, such as the nonlinearity, sensitivity scale factor variation over temperature and power supply noises [12].

Table 1: The Gyroscope's Parameter of MPU9150

Parameter	Type	Units
Sensitivity Scale Factor Variation Over Temperature	±2	%
Nonlinearity	0.2	%
Power-Supply Sensitivity (1-10Hz)	0.2	%

According to the Table 1, the power supply sensitivity and nonlinearity are small. Hence, the main bias of gyroscope is caused by temperature drift. The gyroscope has a process of self-heating when the power is on [13]. During the process, the bias increases with the temperature. However, the process usually takes few minutes. Thus, the bias increases slowly, and when the self-heating completed, the bias can be considered as a constant.

The error of magnetometer is mainly caused by surrounding environment, including temperature, hard irons and soft irons [14]. These factors will lead to a nonlinear variation of magnetic field when yaw changes from -180° to 180°. In this paper, the magnetometer data is involved to correct yaw. Therefore, only X and Y of magnetometer are calibrated. The correction steps are as follows:

1) Rotate the device from -180° to 180°, and find the maximum and minimum values of X and Y: $X_{\max}$, $X_{\min}$, $Y_{\max}$, $Y_{\min}$.

2) Calculate the scale factor X_s, Y_s and bias offsets X_b, Y_b as

$$\begin{cases} X_s = 1 \\ Y_s = \dfrac{X_{\max} - X_{\min}}{Y_{\max} - Y_{\min}} \\ X_b = X_s\left[0.5(X_{\max} - X_{\min}) - X_{\max}\right] \\ Y_b = Y_s\left[0.5(Y_{\max} - Y_{\min}) - Y_{\max}\right] \end{cases} \tag{11}$$

3) The corrected output is given by

$$\begin{cases} X_{out} = X_s X_{in} + X_b \\ Y_{out} = Y_s Y_{in} + Y_b \end{cases} \tag{12}$$

where X_{in}, Y_{in} are the data reading from magnetometer, respectively. X_{out}, Y_{out} are the corrected outputs, respectively.

3.2 Kalman Filter Model

The body rotation of a micro quadrotor and the sensor bias are of crucial importance to determine the orientation. Therefore, the quaternion, the accelerometer bias and the magnetometer bias are included in the state vector. The state equation is described as [2]

$$\begin{aligned} x(k+1) &= \begin{bmatrix} q(k+1) & b_a(k+1) & b_m(k+1) \end{bmatrix}^T \\ &= \Phi(k)x(k) + w(k) \\ &= \begin{bmatrix} \varphi(k) & 0 & 0 \\ 0 & I & 0 \\ 0 & 0 & I \end{bmatrix} x(k) + \begin{bmatrix} w_q(k) \\ w_a(k) \\ w_m(k) \end{bmatrix} \end{aligned} \tag{13}$$

where $\Phi(k)$ is the transition matrix. $w_q(k)$ is given by

$$\begin{aligned} w_q(k) &= -\frac{T_s}{2}\Xi(k)v_g(k) \\ &= -\frac{T_s}{2}\begin{bmatrix} [e(k)\times] + q_0(k)I \\ -e(k)^T \end{bmatrix}\eta_g(k) \end{aligned} \tag{14}$$

On the other hand, $w_a(k)$ and $w_m(k)$ are the process noises with zero mean values and covariance matrices $T_s\sigma_a^2 I$ and $T_s\sigma_m^2 I$, respectively. Assume that $w_q(k)$, $w_a(k)$ and $w_m(k)$ are unrelated. Then, the process noise covariance matrix $Q(k)$ can be expressed as

$$Q(k) = \begin{bmatrix} (T_s/2)^2\Xi(k)\sigma_g^2\Xi(k)^T & 0 & 0 \\ 0 & T_s\sigma_a^2 I & 0 \\ 0 & 0 & T_s\sigma_m^2 I \end{bmatrix} \tag{15}$$

The output vector involves the accelerometer and magnetometer measurement, and the observation equation is

$$\begin{aligned} z(k+1) &= \begin{bmatrix} a(k+1) & m(k+1) \end{bmatrix}^T \\ &= F(x(k+1)) + v(k+1) \\ &= \begin{bmatrix} C_n^b(q(k+1)) & 0 \\ 0 & C_n^b(q(k+1)) \end{bmatrix}\begin{bmatrix} a_0 \\ m_0 \end{bmatrix} \\ &\quad + \begin{bmatrix} b_a(k+1) \\ b_m(k+1) \end{bmatrix} + \begin{bmatrix} v_a(k+1) \\ v_m(k+1) \end{bmatrix} \end{aligned} \tag{16}$$

where a_0 and m_0 are the reference geomagnetism and acceleration vector, respectively.

The covariant matrix of observation noise is

$$R(k+1) = \begin{bmatrix} \sigma_a^2 I & 0 \\ 0 & \sigma_m^2 I \end{bmatrix} \tag{17}$$

4 Robust Extended Kalman Filter Method

Because of the nonlinearity of the observation equation, the following Jacobian matrix should be computed firstly:

$$J = \frac{\partial F}{\partial x} \tag{18}$$

where J is a 6×10 matrix, and for example, $J(1,1)$ can be calculated by

$$J(1,1) = \begin{bmatrix} 2q_1 - C_n^b(1,1)q_1 \\ 2q_2 - C_n^b(1,2)q_1 \\ 2q_3 - C_n^b(1,3)q_1 \end{bmatrix}^T a(k) \tag{19}$$

The steps of proposed robust extended Kalman filter are summarized as follows [2]:

a) Calculate the priori state estimate:

$$x^-(k+1) = \Phi(k)x(k) \tag{20}$$

b) Calculate the priori error covariance matrix:

$$P^-(k+1) = \Phi(k)P(k)\Phi(k)^T + Q(k) \tag{21}$$

c) Calculate the Kalman gain:

$$K(k+1)=P^{-}(k+1)J^{T}(k+1)\\ [J(k+1)P^{-}(k+1)J^{T}(k+1)\\ +R(k+1)L(k+1)]^{-1} \quad (22)$$

where L is the weight matrix.

d) Calculate the posteriori state estimate:

$$x(k+1)=x^{-}(k+1)+K(k+1)\\ \{z(k+1)-F[x^{-}(k+1)]\}^{-1} \quad (23)$$

e) Calculate the posteriori error covariance matrix:

$$P(k+1)=P^{-}(k+1)-K(k+1)F(k+1)P^{-}(k+1) \quad (24)$$

In (24), the weight matrix $L(k+1)$ can be a diagonal matrix with the elements blew:

$$l_i(k+1)=\begin{cases}1 & ,\left|\dfrac{V_i(k+1)}{\sigma_i}\right|<c\\ \dfrac{|V_i(k+1)/\sigma_i|}{0.2c} & ,\left|\dfrac{V_i(k+1)}{\sigma_i}\right|>c\end{cases} \quad (25)$$

where c is a constant between 1.3 and 2, $V(k)=z(k)-F[x^{-}(k)]$ is the residual of observation, $V_i(k+1)$ is the i th element of $V(k)$, and σ_i is the i th diagonal element of $R(k+1)$.

The priori state estimate $x^{-}(k+1)$ is predicted by the previous posteriori state $x(k)$ firstly. Then, $x(k+1)$ is updated by Kalman gain $K(k+1)$ and residual $V(k)$. After estimating the posteriori state $x(k+1)$, the quaternion $q(k+1)$ is obtained, and the Euler angle can be calculated by (9).

5 Experiments and Simulations

5.1 The self-designed micro quadrotor

The experiment was carried out on a self-developed micro quadrotor platform XiaoxinV2:

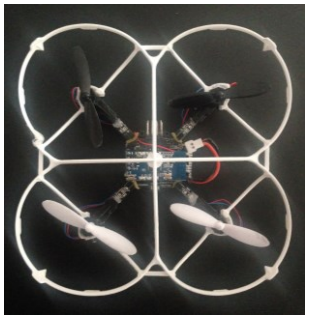

Fig.1: A self-designed micro quadrotor platform

The platform includes a flight control system, a power system, a driving system, a communication system, and a protection system.

The flight control system employed a Cotex-M4 core MCU, which has a frequency up to 168MHz, a build-in float point unit (FPU), and a special digital signal processing (DSP) library. The IMU is MPU9150, which contains a tri-axis gyroscope, a tri-axis accelerometer and a tri-axis magnetometer in one chip. Thus, the coaxiality is better than the scheme like MPU6050+HMC5883.

A 350mAh lithium battery is fixed beneath the body to supply electric power. When there is no extra load, a maximal flight time is up to 7 minutes.

Four 720 coreless motors are driven by metal oxide semiconductor field effect transistor (MOSFET) to provide lift. Considering the scale, 55 mm rotor is chosen to match the motor. The rotate speed range is divided into 500 levels, which can provide enough accuracy for control.

The platform can communicate with the ground station and remote device through Zigbee. Restricted by the volume, the antenna is printed on the circus board. The effective distance is 150 m.

The micro quadrotor is surrounded by a protection cage, which can protect rotor from top and side. Four sleeves are employed to fixed the rotor and avoid the crash from bottom.

5.2 The Correction of Magnetometer

Rotate the micro quadrotor for 360° , we obtain the raw X and Y data of magnetometer:

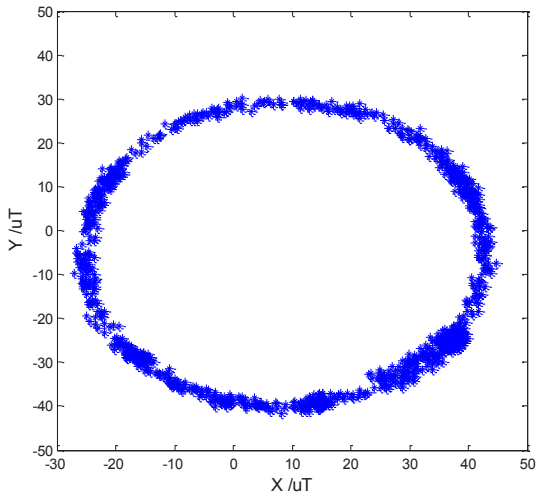

Fig.2: Magnetometer before correction

Then, the correction output can be determined:

$$\begin{cases}X_{out}=X_{in}-8.85\\ Y_{out}=0.9974Y_{in}+5.6533\end{cases} \quad (26)$$

The output after correction is shown in Fig.3.

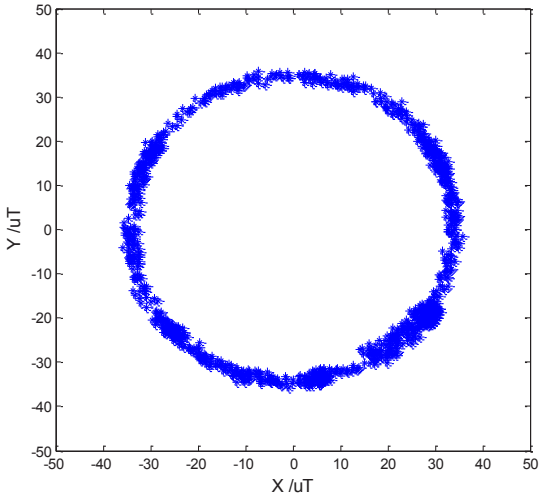

Fig.3: Magnetometer after correction

After correction of magnetometer data, the figure of data changes from eclipse to circle, and the center is moved to the origin.

5.3 Simulation Results

The attitude estimation frequency is fixed at 200Hz, and the sample frequency of MPU9150 is set at 200Hz too.

The simulation parameters are as follows:

a) The geomagnetism in Nanjing has a vertical component as $3.48\times10^{-5}T$ and a horizontal component as $3.31\times10^{-5}T$. And the magnetic declination is 4°. The reference geomagnetism vector is:

$$m_0 = \begin{bmatrix}0.243 & 3.47 & 3.31\end{bmatrix}^T \times 10^{-5}T \tag{27}$$

b) The reference acceleration vector can be determined when the platform is horizontal.

$$a_0 = \begin{bmatrix}0 & 0 & 1\end{bmatrix}^T \tag{28}$$

c) The initials conditions of Kalman filter are:

$$q(0) = \begin{bmatrix}1 & 0 & 0 & 0\end{bmatrix}^T \tag{29}$$

$$P_0 = diag(0.0014, 0.0016, 0.0014, 0.0016) \tag{30}$$

$$Q = diag(0.01, 0.01, 0.01, 0.01) \tag{31}$$

$$R = diag(10, 10, 10, 20, 20, 20) \tag{32}$$

d) The constant c in weight matrix L is 1.3.

When the platform is not movement in a certain orientation, the simulation results are shown below:

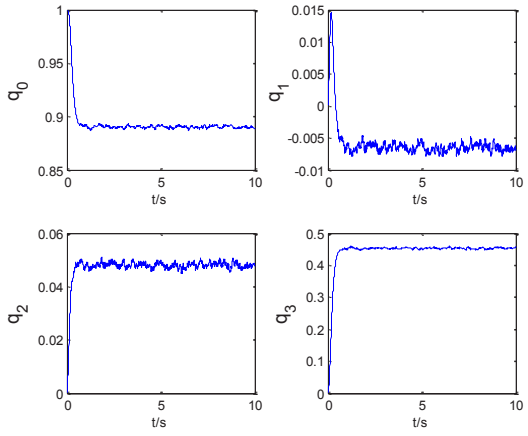

Fig. 4: The quaternion

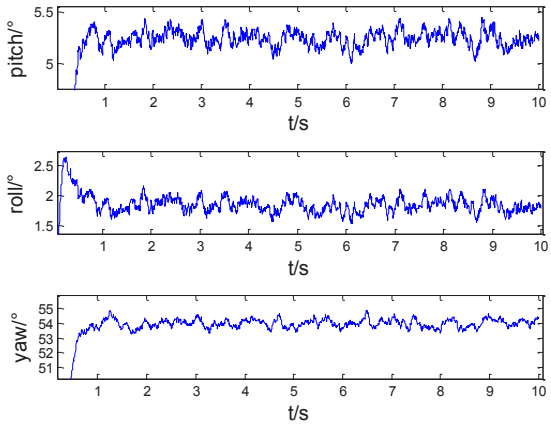

Fig. 5: The Euler angle

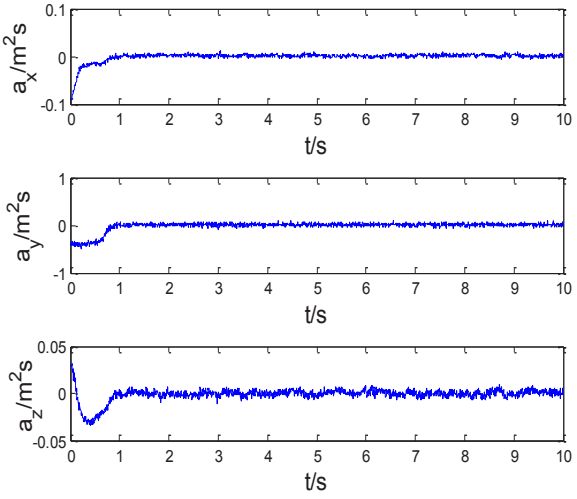

Fig. 6: The estimation error of accelerometer

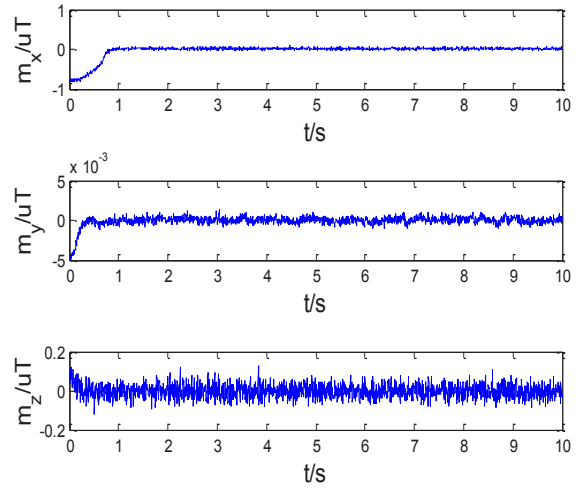

Fig. 7: The estimation error of magnetometer

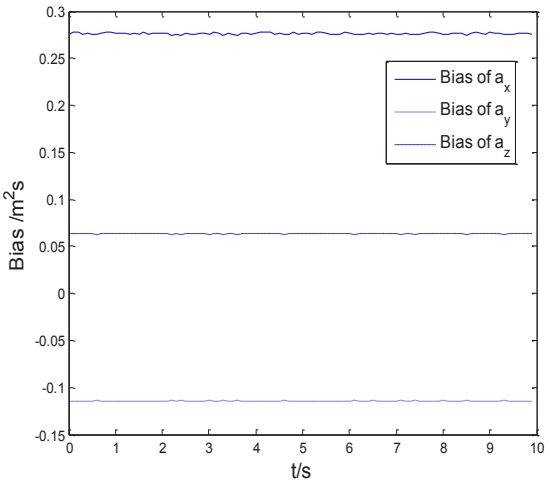

Fig. 8: The bias of accelerometer

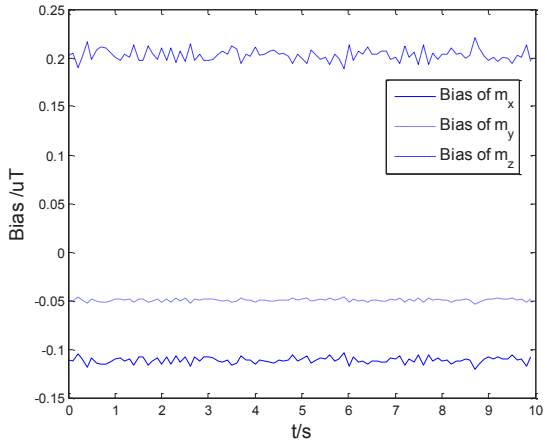

Fig. 9: The bias of magnetometer

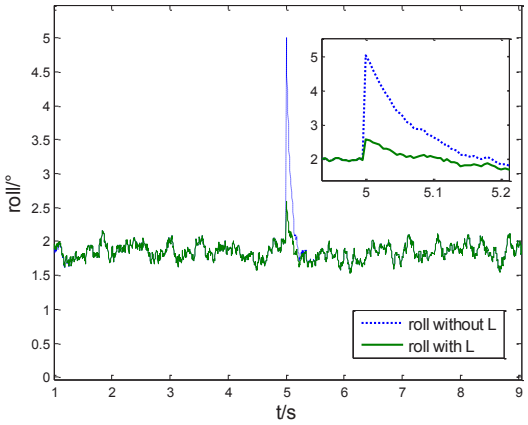

Fig. 10: The roll with observation outliers

As shown in Fig. 4, the quaternion becomes stable very fast, which indicates that the convergence performance of developed Kalman filter is good. Fig. 5 gives the Euler angles calculated by (9), from which the pitch, roll and yaw angles are controlled within $\pm 0.25^{\circ}$, $\pm 0.25^{\circ}$ and $\pm 1.0^{\circ}$, respectively. The error's accumulation is suppressed, and because of the fuse of magnetometer, the continuous increase or decrease of yaw is avoided. The observation error given in Fig. 6 and Fig. 7 demonstrate that the estimation error converges to 0, which indicates a satisfactory precision. Fig. 8 and Fig. 9 present the estimate bias of accelerometer and magnetometer. Although the true bias is unknown, the developed Kalman filter gives the estimate value, which can be used to correct the observation. In Fig. 10, an outlier is injected in a_x at 5s, and the estimate roll shows that weight matrix L can suppress outliers effectively.

6 Conclusion

This paper has presented a quaternion-based robust extended Kalman filter to estimate the attitude of micro quadrotor using low-cost MEMS. In each iteration, the posteriori state estimate gives both the quaternion and sensor bias, which can be used to calculate the Euler angle and compensate the sensor's output conveniently. The estimate errors all converge to 0 and the influence of outliers is suppressed. The fuse of magnetometer solves the drift of yaw, and the calibration of magnetometer ensures its accuracy. The experiment carried out on the self-designed micro quadrotor shows a good real-time performance, and the attitude obtained by the prospered method is reliable for further control law design.

References

[1] Y. Mulgaonkar, Design of small, safe and robust quadrotor swarms. *Robotics and Automation (ICRA) IEEE International Conference on IEEE*, 2015.

[2] A. M. Sabatini, Quaternion-based extended Kalman filter for determining orientation by inertial and magnetic sensing, *IEEE Transactions on Biomedical Engineering*, 53(7):1346-1356, 2006.

[3] E. A. Wan, The Unscented Kalman Filter for Nonlinear Estimation, *Adaptive Systems for Signal Processing, Communications, and Control Symposiu*. 153-158, 2000.

[4] S. J. Julier, A New Extension of the Kalman Filter to Nonlinear Systems. *Proceedings of SPIE - The International Society for Optical Engineering*, 3068:182-193, 1999.

[5] J. L. Crassidis, Unscented Filtering for Spacecraft Attitude Estimation[J]. *Journal of Guidance Control & Dynamics*, 26(4):536-542, 2003.

[6] C. Tsai, An adaptive robustizing approach to kalman filtering, *Automatica*, 19(3):279-288, 1983.

[7] K. R. Koch, Robust Kalman filter for rank deficient observation models. *Journal of Geodesy*, 72(7-8):436-441, 1998.

[8] X. Kong, Robust Kalman filtering for attitude estimation using low-cost MEMS-based sensors, *Guidance, Navigation and Control Conference (CGNCC), 2014 IEEE Chinese. IEEE*, 2014:2779-2783.

[9] E. Fresk, Full quaternion based attitude control for a quadrotor, *Control Conference (ECC)*, 2013 European. IEEE, 2013:3864-3869.

[10] X. Zhang, Kalman Filtering of Attitude Measurement with Magnetometer and Gyroscope. *Journal of Detection & Control*, 2011, 33(4):48-43.

[11] J. H. Liang, W. C. Wang, T. M. Wang. Design of AHRS Based on ARM and Low-cost MEMS Devices[J]. *Microcontrollers & Embedded Systems*, 2012.

[12] InvenSense Inc, MPU-9150 Product Specification Revision 4.3. 2013.

[13] H. Abbott, Land-vehicle navigation using GPS, *Proceedings of the IEEE*, 1999, 87(1):145-162.

[14] M. J. Caruso, Applications of magnetic sensors for low cost compass systems, *Position Location and Navigation Symposium, IEEE*, 2000:177 - 184